Proceedings of the IASS 2024 Symposium
Redefining the Art of Structural Design
August 26-30, 2024, Zurich, Switzerland
Philippe Block, Giulia Boller, Catherine DeWolf,
Jacqueline Pauli, Walter Kaufmann (eds.)

Interdisciplinary optimisation tool for doubly curved beam-like shell floors made of CFRP prestressed concrete

Jamila LOUTFI*, Max DOMBROWSKI[a], Paul MERZ[b], Ahmad EIZ EDDIN[a], Mike SCHLAICH[a]

* TU Berlin, Institute of Civil Engineering, Chair of Conceptual and Structural Design
Berlin University of the Arts, Department for Structural Design and Engineering,
Hardenbergstraße 33, 10623 Berlin, Germany
j.loutfi@udk-berlin.de

[a] TU Berlin, Institute of Civil Engineering, Chair of Conceptual and Structural Design
[b] ETH Zürich, Institute of Structural Engineering, Chair of Structural Engineering – Concrete Structures and Bridge Design

Abstract

This paper explores the interdisciplinary design of hyperbolic paraboloid (HP) shell floors using precast elements constructed with carbon-fibre-reinforced polymer (CFRP) prestressed concrete. An optimisation tool is introduced, taking into account the ultimate and serviceability limit state as well as sound insulation. The optimisation tool is structured in (i) input parameters, (ii) an analysis model to determine the relevant properties of the system, (iii) design checks to compile a penalty function, (iv) the calculation of the objective values global warming potential (GWP) and material costs, and (v) an objective function that combines the penalty function and the objective values. An optimisation algorithm is implemented that varies the input parameters to minimise the objective function, thereby identifying the most GWP- and cost-efficient shell designs. Single-objective optimisations are performed to attain insights into the influence of different input parameters and design checks on the optimisation outcomes. Additionally, a multi-objective optimisation considering GWP and costs is performed to evaluate the trade-off between both objectives. Initial indications suggest, that the fitness functions of these two objective values are largely aligned and that no Pareto problem arises. The optimisation model introduced in this paper can be used to gain comprehensive insights into the interdisciplinary design of HP shell floors for the design of material-efficient structures.

Keywords: HP shells, concrete shells, parametric design, embodied carbon, material costs, load-bearing capacity, moment-curvature relationship, sound insulation, genetic algorithm, structural optimisation

1. Introduction

The construction and building sector is responsible for 38% of global greenhouse gas emissions [1], while at the same time, steady population growth and rapid urbanisation are driving the construction of buildings. In this context, the structural optimisation of floor systems offers great potential, as floors account for around 40% of greenhouse gas emissions of an average building [2]. The present work deals with the design of hyperbolic paraboloid (HP) shells made of carbon-fibre-reinforced polymer (CFRP) prestressed concrete as resource-efficient floor elements. A digital optimisation tool is presented that can be used to gain insights into the design space of these elements.

HP shells made from steel-reinforced and steel-prestressed concrete were extensively used as a roof system during the 1960s and 1970s, e.g. in Germany [3]. The concept was reintroduced in [4] with

the suggestion to use HP shells as modular beam-like elements for material-efficient floor systems and is further developed in this paper by some of the authors. Due to their anticlastic double-curvature, HP shells possess a very efficient load-bearing behaviour, allowing for significant material reduction compared to conventional flat slabs. To minimise concrete cover and cross-sections, corrosion-resistant CRFP is used as textile reinforcement. Due to the exceptionally high strength of CRFP, very small reinforcement cross-sections are required, leading to overall low bending stiffness and large deflections under service loads. However, research at TU Berlin has shown that prestressing can effectively limit the deflections of thin-walled CFRP-reinforced elements [5, 6, 7]. As doubly ruled surfaces, HP shells can be prestressed very effectively, using their two sets of straight generatrices.

Because HP shells were primarily used as roof elements in the past, their design as floor elements is still largely unknown. Unlike roofs, floor elements require additional verifications such as fire resistance and sound insulation. Shells, with their thin cross-section, are particularly sensitive to such phenomena as well as structural concerns like deformations, stability, and vibration issues. Additionally, material-efficient shells possess highly utilized cross-sections, which makes them sensitive to minor changes in input parameters. Altogether, the design of HP shell floors is a complex problem that involves interdisciplinary requirements with partly counteracting effects on the design outcome.

Dealing with complex design problems, designers often face the challenge of reconciling competing or conflicting requirements of different disciplines, which complicates their understanding of how various design parameters interrelate and influence optimal design outcomes [8]. To get a better understanding of a design space and its unique features, single- and multi-objective optimisation tools can be used to study the influence of certain input parameters, boundary conditions and other meta-parameters on the design outcomes.

The aim of the present work is to develop an interdisciplinary and automated optimisation tool for the design of HP shells made of CFRP prestressed concrete. The first steps are taken by introducing essential structural design checks for pre-dimensioning along with sound insulation requirements, thereby showcasing the tool's interdisciplinary capabilities. To explore the design space, single- and multi-objective optimisation is performed, and different objective values are implemented to evaluate the influence of the various input parameters on the design outcome.

2. Interdisciplinary optimisation tool for HP shell floors

The optimisation tool was developed within the visual programming environment "Grasshopper 1.0.0007" and contains the following steps as shown in Figure 1: (1) definition of input parameters including materials, geometric properties and loads, (2) determination of relevant properties regarding structural and sound insulation properties in the analysis model, (3) design checks to evaluate the feasibility of the design (4) determination of the two considered objective values GWP and costs, and (5) calculation of the objective function by combining the objective values with penalty values based on the unfulfilled design checks. An optimisation algorithm (6) is applied to vary the input parameters in order to minimise the objective function.

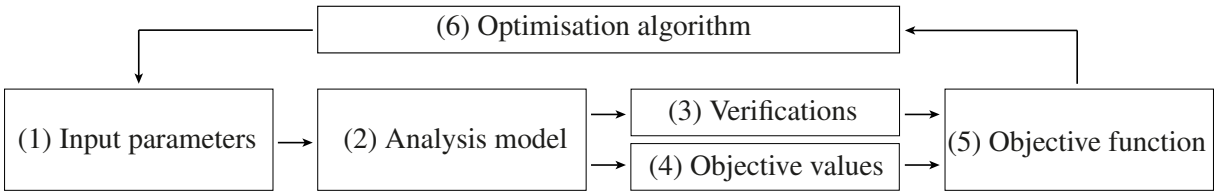

Figure 1: Flow chart of the optimisation tool

2.1. Input parameters

The HP shell design is determined by a specific set of geometric and material-specific parameters as well as design requirements. The composition of the HP floor system and the relevant geometric parameters are shown in Figure 2.

Some of the input variables, the so-called design parameters, remain constant during the optimisation runs. The remaining input variables are varied by the optimisation algorithm and are termed optimisation parameters. These include the shell thickness t, the number of tendons n_{t}, the edge distance dy, the concrete quality, the degree of prestressing and the cross-section area of a tendon A_{tex} (see Figure 3).

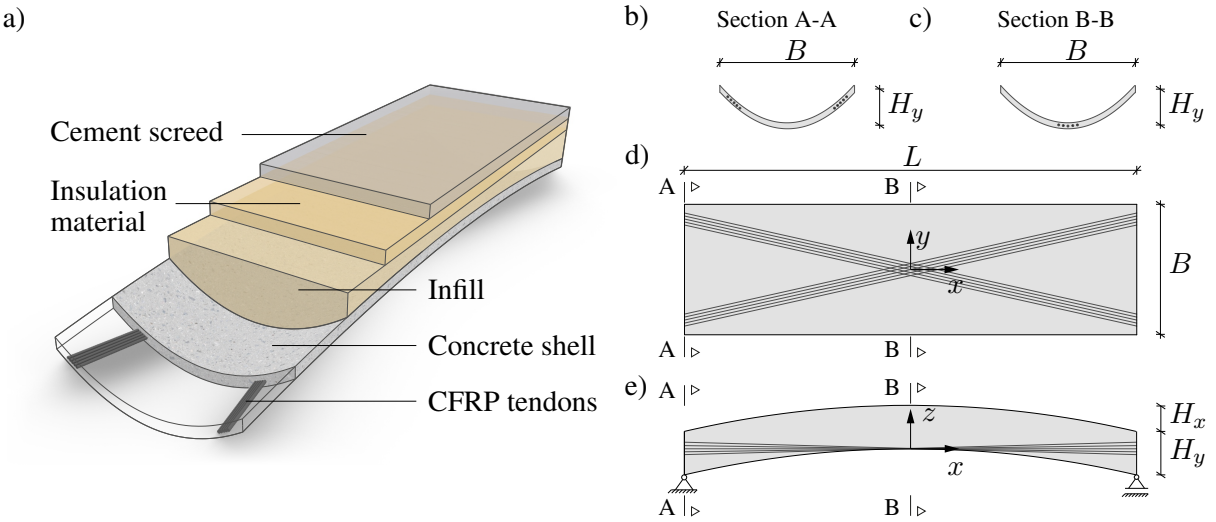

Figure 2: HP beam-like shell floor element: (a) rendering of HP floor element with its material layers, (b) cross-section at support and (c) at mid span, (d) top view and (e) side view

2.2. Analysis model

Analytical descriptions for the structural geometry and its properties were derived to shorten the runtime compared to finite element simulations. The next paragraphs give an insight into the analysis model.

2.2.1. Geometry generation

The mathematic generation of the HP shells mid surface is defined by a translational surface, set up by a parabolic curve translated along a perpendicularly oriented parabolic curve with opposite curvature (see Figure 3 a). The relation between the vertical dimensions H_x and H_y has a strong influence on the magnitude of internal forces in longitudinal and transverse direction [4].

$$z = \frac{y^2}{b^2} - \frac{x^2}{a^2}; \qquad a = \frac{L}{2 \cdot \sqrt{H_x}}; \qquad b = \frac{B}{2 \cdot \sqrt{H_y}} \tag{1}$$

A different geometric description focusing on the straight generatrices in the doubly ruled surface is used to determine the tendon layout. Introducing the parameter α along the edges of the hyperbolic paraboloid as shown in Figure 3 b), the straight lines can be mathematically expressed with:

$$\vec{x}(x) = \begin{pmatrix} x \\ \frac{x}{x_{\text{p}}} \cdot y_{\text{p}} \\ \frac{x}{x_{\text{p}}} \cdot (4\alpha - 2) \cdot z_{\text{p}} \end{pmatrix} + \begin{pmatrix} 0 \\ (2\alpha - 1) \cdot y_{\text{p}} \\ (4\alpha^2 - 4\alpha + 1) \cdot z_{\text{p}} \end{pmatrix} \tag{2}$$

Any point on a generatrix is defined by the global coordinate x and the coordinates x_p, y_p and z_p that describe the corner points P_x^+, P_y^+, P_x^- and P_y^- of the hyperbolic paraboloid. The tendons for pre-stressing the HP shell are anchored at the short edges of the surface and the centre tendons run through the coordinate origin (saddle point) of the HP shell. The red highlighted area in Figure 3 represents the available area for the tendon layout, which is influenced by the geometry parameters of the HP shell.

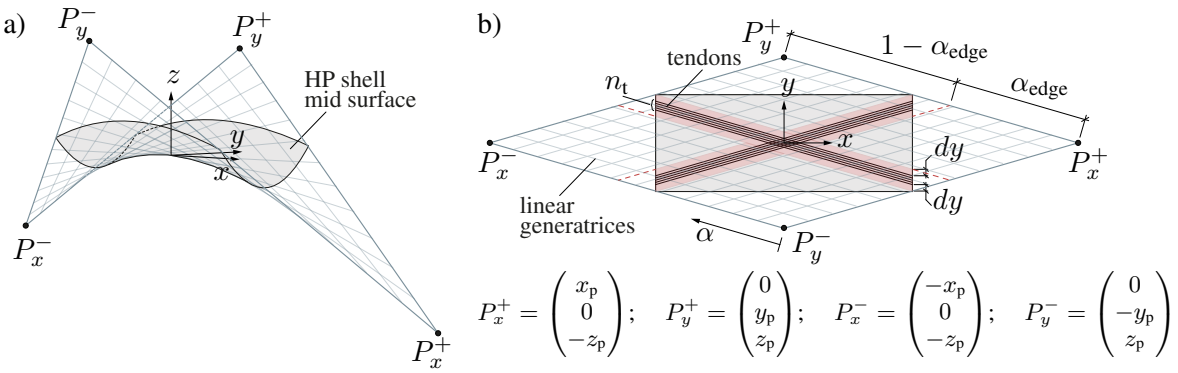

Figure 3: Overiew of the geometry and tendon layout of the HP shell: (a) perspective and (b) top view of HP shell mid surface and its linear generators described by four corner points P_x+, P_y+, P_x- and P_y- and parameter α; illustration of possible tendon distribution between short edges with parameters n_t and dy within the geometrically available tendon area highlighted in red

The number of CFRP tendons, n_t, and the distance of the outermost tendon towards the edge point, dy, are introduced as two input parameters. They are combined into the variable α_edge that is evaluated in Equation 3 to generate the linear parameterisation of the tendon layout.

$$\alpha_\mathrm{edge} = \begin{cases} 0.5, & \text{if } n_\mathrm{t} = 1 \\ \frac{1}{2}\left(\frac{0.5 \cdot B - dy}{y_\mathrm{p}} - \frac{x}{x_\mathrm{p}} + 1\right), & \text{if } n_\mathrm{t} \geq 2 \end{cases} \tag{3}$$

2.2.2. Load-bearing behaviour

Following the assumption that the HP shell can be regarded as a simply supported beam along the longitudinal axis, the bending capacity and deformation behaviour can be determined through cross-sectional analysis. To do this, the parabolic cross-section shown in Figure 4 e) is defined with the local coordinate $\overline{z}$. To compute the bending capacity of the cross-section, the stress-strain curve for concrete in ultimate limit state (ULS) according to DIN EN 1992-1-1:2004 + AC:2010 is used (see Figure 4 d). Based on the defined local coordinate system, the stress function can be expressed as follows:

$$\sigma(\overline{z}) = \begin{cases} f_\mathrm{cd}, & \text{if } \overline{z} \leq \overline{z}_\mathrm{r} \\ \left(\frac{-f_\mathrm{cd}}{h_\mathrm{p}^2}\right) \cdot (\overline{z} - \overline{z}_\mathrm{r})^2 + f_\mathrm{cd}, & \text{if } \overline{z}_\mathrm{p} \geq \overline{z} \geq \overline{z}_\mathrm{r} \end{cases} \tag{4}$$

The bending capacity of the HP shell is computed using the iterative Regula-Falsi method to determine the strain state of the cross-section. Since both a compression failure of the concrete and a tensile failure of the CFRP are possible, the assumption of tensile failure is used as an initial condition. In this strain state, the outermost CFRP fibre possesses its maximum strain and the according strain of concrete at the compression edge is varied until the inner forces of the cross-sections are in equilibrium. If no equilibrium is found this way, the initial condition has to be changed to compression failure and the strain in the outermost CFRP has to be iterated. For each strain state, the determination of the internal forces

of the CFRP tendons and their centroid can be easily derived from the linear stress-strain relationship. To determine the internal compression force of the concrete and its centroid, the nonlinear stress-strain curve has to be integrated over the parabolic geometry of the cross-section. This only yields a closed solution for the bending capacity in ULS for normal concrete. For SLS or if high-strength concrete is used, only iterative solutions can be derived. Once the strain state in equilibrium is found, the bending capacity can be computed using the inner forces of concrete and CFRP and their lever arms.

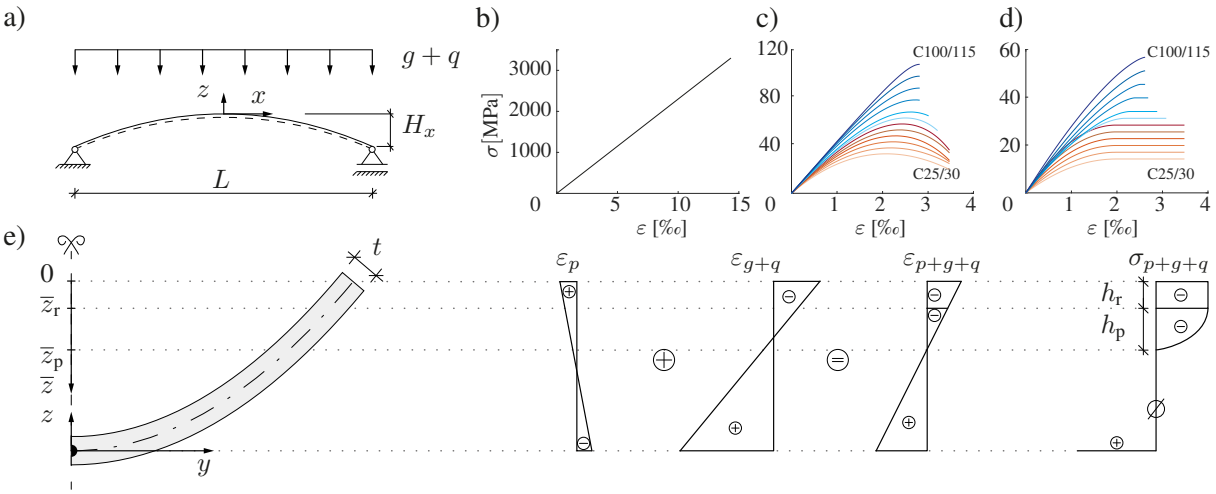

Figure 4: Overview of the analysis model for load-bearing and deformation behaviour: (a) single-span beam with global coordinate system and uniform loads, (b) linear stress-strain curve of CFRP, (c) non-linear and (d) parabolic-rectangular stress-strain curve of concrete according to DIN EN 1992-1-1:2004 + AC:2010, (e) strain and stress distribution of a parabolic cross-section with $n_t = 1$ tendons in ULS subjected to bending and prestressing, considering normal strength concrete

2.2.3. Deformation behaviour

The deflection of the system is analysed using the moment-curvature diagram in combination with the force method. The prestressing is considered as a strain state with the resulting pre-curvature from the eccentricity of the tendon resulting in a moment M_p under prestress as shown in Figure 5.

The position of the tendons within the constant concrete cross-section changes along the longitudinal direction, which leads to changes in the failure moment M_u, cracking moment M_{cr} and moment under prestressing M_p. Due to the parabolic geometry in the longitudinal direction, the lever arm changes in an approximately quadratic manner. Therefore, parabolic functions were introduced to approximate M_u, M_{cr} and M_p, reducing the required cross-sectional analyses to only mid-span and support. In Figure 5, the defined parabolic functions for an HP shell design show a good approximation compared to the results of cross-sectional analyses carried out at multiple steps along the length.

2.2.4. Sound insulation

In the optimisation tool, the airborne sound reduction index R_w and the normalised impact sound pressure level L_{nw} are determined with a simplified approach, considering the HP floor system as a rectangular cross-section. Following this approach, the acoustic properties can be determined by the mass per unit area of the HP shell and the infill layer according to DIN 4109-32:2016-07. A current approach to examine the acoustic behaviour of HP shell floors using extensive numerical simulations and regression functions can be found in [9]. The approach considers more variables to compute the acoustic properties than the simplified normative approach and it can be easily integrated into the present optimisation tool. However, laboratory measurements are still necessary, to verify the method.

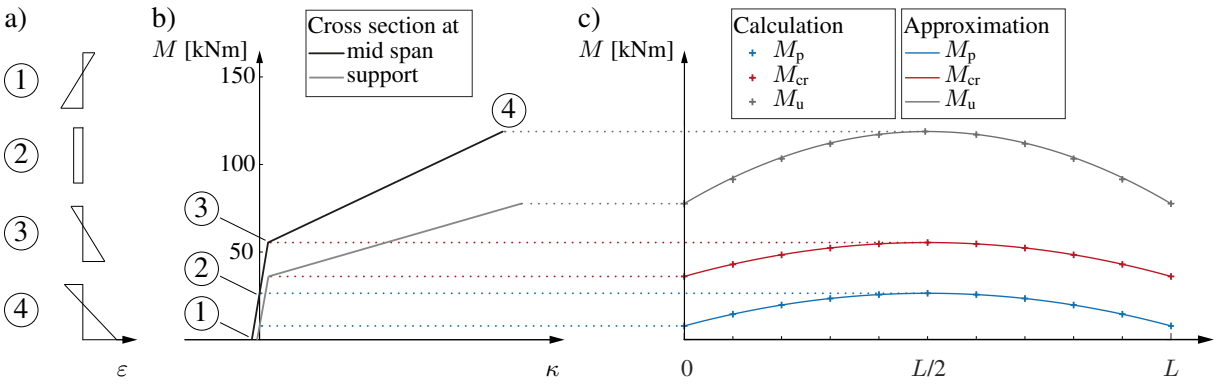

Figure 5: Moment-curvature relationship of the reference HP shell design (see section 3.): (a) strain distribution of cross-section for the states of (1) prestressing, (2) zero curvature, (3) first crack and (4) failure, b) moment-curvature diagram for cross-section at mid span and at supports, (c) calculated values and approximated development of M_p, M_cr and M_u for different cross-sections along the span L

2.3. Design checks

The design checks included in the current version of the tool are summarised in Table 1. Regarding structural design checks in ULS, bending capacity at mid span is implemented. For SLS, deformation limitation and failure warning are implemented based on deformation targets used in [7]. Furthermore, structural requirements including bar spacing, concrete cover and minimum shell thickness depending on the tendon's diameter d_p are introduced to obtain buildable results, here based on [10]. For the acoustic requirements, the airborne sound and impact sound insulation are verified according to DIN 4109-2:2018-01. For each set of input parameters, the utilisation rates η_i of all design checks are determined and converted into penalty values p_i (see Equation 5).

Table 1: Design checks implemented in the optimisation tool

Category	Label	Design Check	Formula
ULS	A.1	Bending load-bearing capacity	$M_\mathrm{Ed} \leq M_\mathrm{Rd}$
SLS	B.1	Deformation limitation	$w_\mathrm{max} \leq L/f_\mathrm{B.1}$
	B.2	Failure warning	$w_\mathrm{max} \geq L/f_\mathrm{B.2}$
Structural requirements	C.1	Minimum concrete cover	$c_1 \geq c_\mathrm{nom} = 3 \cdot d_\mathrm{p}$
	C.2	Minimum bar spacing	$s \geq s_\mathrm{req} = 5,75 \cdot d_\mathrm{p}$
	C.3	Minimum shell thickness	$t \geq 2 \cdot c_\mathrm{nom} + 2 \cdot d_\mathrm{p} + s_\mathrm{req}$
Building physics requirements	D.1	Airborne sound reduction index	$R_\mathrm{w} \geq R_\mathrm{w,req} + 2\,\mathrm{dB}$
	D.2	Normalised impact sound pressure level	$L_\mathrm{nw} \leq L_\mathrm{nw,per} - 3\,\mathrm{dB}$

2.4. Objective values

Two crucial objectives for the design of floor elements are the GWP and the costs. However, the modular structure of the optimisation tool makes it possible to use any value derived from the tool's data as an objective value. The scope of the life cycle assessment (LCA) based on the standard DIN EN 15978:2012-10 is defined to include stages A1-A3 as those stages allow for good data availability and do not rely on end-of-life scenarios and project-specific boundary conditions. The optimisation tool

considers only material costs since transportation and construction costs are more project-specific and have a significantly lower impact on the final costs [11]. The material database for the optimisation tool includes the GWP and material costs values, as shown in Figure 7 b). The resulting objective values for GWP and costs are normalized by the net floor area of the floor element.

For the following analyses, the embodied carbon and the material costs of the infill, the sound insulation layer, and the cement screed are neglected. A more detailed approach for these components was incorporated into an updated version of the optimisation tool by Eiz Eddin [9].

2.5. Objective function

The fitness function $f(\overline{x})$ for a parameter combination $\overline{x}$ is defined as follows:

$$f(\overline{x}) = Z \cdot \prod_{i=1}^{n} p_i\left(\eta_i\right)^2 \qquad \text{with } p_i\left(\eta_i\right) = \begin{cases} 1, & \text{if } \eta_i \leq 100\% \\ \eta_i, & \text{if } \eta_i > 100\% \end{cases} \tag{5}$$

with an objective value Z, the penalty values p_i, the utilisation rates η_i and the amount of checks n.

2.6. Optimisation algorithm

The optimisation algorithm varies the optimisation parameters in order to minimise the objective function. In the optimisation tool, the plug-in Galapagos in Grasshopper is used to solve single-objective problems. As a result of benchmark tests, a maximum stagnant of 50, a population of 80 individuals, an initial boost of 30, a maintain of 10% and an inbreeding of 50% were defined for the optimisation runs. Three optimisation runs were carried out for each optimisation test. The parameter combination with the lowest fitness value is selected from the three results, irrespective of the objective value.

Additionally, the Octopus plug-in Grasshopper can be used to solve multi-objective optimisation problems. In this case, multiple objective functions as defined in Equation 5 can be used. This enables to evaluate the interaction and trade-offs between multiple objective values [12]. The default parameters of Octopus with a population of 100 individuals, a mutation probability of 0.2 and a mutation rate of 0.9 were used for the optimisation runs.

3. Results

For this research paper, single- and multi-objective optimisations were carried out, based on a reference design with the design parameters $L = 8.00\,\text{m}$, $B = 1.00\,\text{m}$, a total height of $H_{\text{tot}} = 0.40\,\text{m}$ and $H_x/H_y = 0.2$.

3.1. Single-objective optimisation

The following boundary conditions were defined for the single-objective optimisation runs: live load $q = 3\,\text{kN/m}^2$, deformation limitation factor $f_{\text{B.1}} = 250$, failure warning factor $f_{\text{B.2}} = 100$, sound reduction index $R_{\text{w}} = 53\,\text{dB}$ and permitted impact sound level $L_{\text{nw}} = 53\,\text{dB}$.

The results in Figure 6 show the GWP and GWP fitness values for the optimum designs (left) with its associated utilisation rates of different design checks (right). The reference design possesses a GWP and GWP fitness value of around $18.2\,\text{kg}\,\text{CO}_2\text{eq/m}^2$.

For smaller spans, the GWP and GWP fitness value are lower, and by raising the span L, both values increase. Few gaps between both graphs are visible which is related to optimal designs with not fulfilled design checks such as deformation limitation (B.1) and minimum shell thickness (C.3). The longer the

HP floor element, the more relevant the deformation limitation design check is, since the deformation increases much faster than the bending moment. This is why the B.1 design check dominates in comparison to A.1. The high utilisation rate of C.3 shows that all optimised designs have a minimal thickness t. The small gaps between GWP and GWP fitness indicate that the penalties are not calibrated perfectly in order to find an optimum that satisfies all design checks.

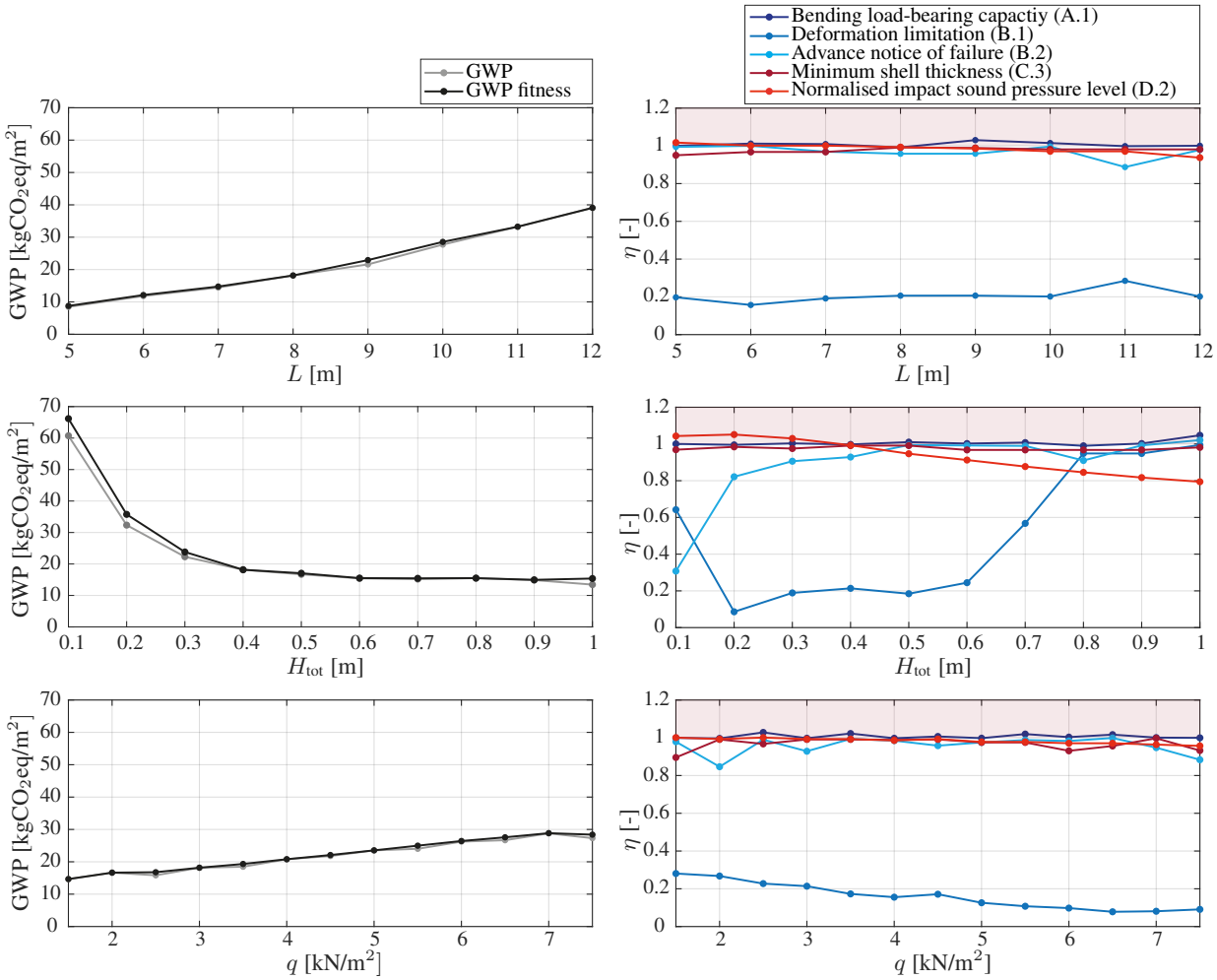

Figure 6: Single-objective optimisation results for objective value GWP by variation of the span L, the total cross-section height H_{tot} and the live load q: Plots of GWP and GWP fitness values (left) and its utilisation rates η of design checks (right)

For the case of varying the total cross-section height H_{tot}, the GWP and GWP fitness values get smaller as H_{tot} increases from 0.1 m to 0.6 m. For the satisfaction of A.1 and D.2 a design with a small H_{tot} would need a greater thickness in order to obtain a greater mass and stiffness. For larger H_{tot} the optimum designs possess enough mass due to a higher volume of infill to satisfy the design check D.2. The gap between GWP and GWP fitness for H_{tot} at 0.1 m and 0.2 m are related to the parameter domain's upper range value of the optimisation parameter t. For all steps of H_{tot}, the ULS and SLS design checks are optimised to have a high utilisation.

By increasing the live load q, the GWP and GWP fitness values increase nearly proportionally. The three design checks, A.1, B.2 and D.2, determine the penalty values of each optimum design, whereas the deformation limitation is irrelevant for the optimum designs.

3.2. Multi-objective optimisation

A small study using the multi-objective optimisation plug-in Octopus was conducted to get a first understanding of the trade-off between GWP and cost. The results of this optimisation are shown in Figure 7.

The dark blue highlighted dots mark the HP designs with complete fulfilment of design checks, whereas all designs shown in grey have at least one utilisation rate greater than 1. A correlation between the GWP and the cost objectives can be observed. No conflicting relationship can be interpreted thus no Pareto front is visible. This preliminary result would mean, that a multi-objective optimisation is not necessary to model the trade-off between GWP and cost.

a)

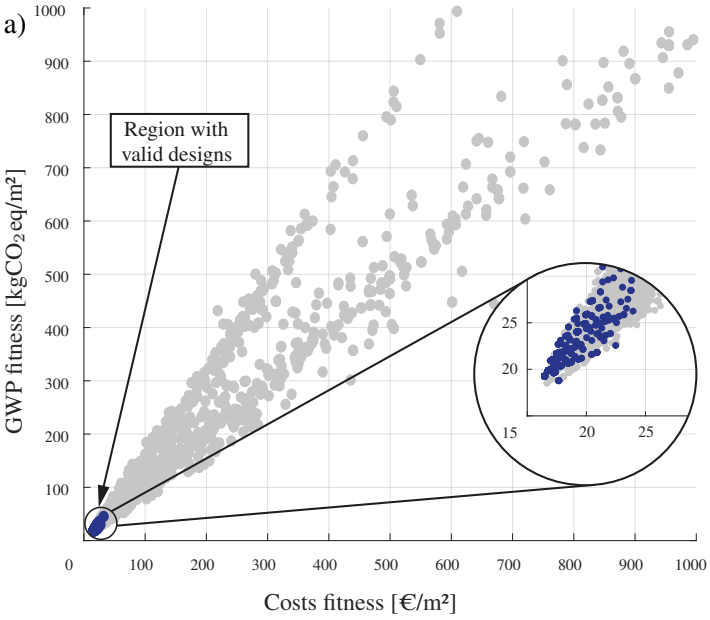

b)

Concrete grade	GWP [kgC0$_2$eq/m³]	Costs [€/m³]
C25/30	197	70
C30/37	219	72.5
C35/45	244	75
C40/50	265 [a]	80
C45/55	286	85
C50/60	300	90
C55/67	314 [b]	100 [b]
C60/75	328 [b]	110 [b]
C70/85	342 [b]	120 [b]
C80/95	356 [b]	130 [b]
C90/105	370 [b]	140 [b]
C100/115	384 [b]	150 [b]

[a] interpolated; [b] extrapolated

CFRP product	GWP [kgC0$_2$eq/kg]	Costs [€/kg]
solidian GRID Q85-CCE-21	23900	49.00

Figure 7: Multi-objective optimisation results: (a) scatter plot of material cost fitness and GWP fitness values; designs with completely fulfilled design checks highlighted in dark blue, (b) applied data of GWP and material costs for 1 m³ concrete [13, 14] and 1 kg CFRP [11, 15]

4. Conclusion

An interdisciplinary optimisation tool for HP shell floors was introduced, that considers the structural and acoustic behaviour of the system, as well as structural constraints. The presented optimisation tool enables rapid examination of various parameter combinations and enables insights into the influence of input parameters, design checks and meta-parameters on the design outcomes.

The tool was used to perform single- and multi-objective optimisations, yielding highly GWP- and cost-efficient designs as reasonable outcomes. Moreover, it was observed that with the current material database and the implemented design checks, an aligning behaviour of both objective values GWP and costs can be observed, which would make multi-objective optimisations redudant.

The present research aims to integrate all relevant aspects of the design of HP shell floors into a single, data-based model. This advances the pragmatic design of material-efficient floor elements for sustainable buildings.

Future steps to close existing gaps could include enhancing the penalty function to avoid the observed gaps and incorporating missing requirements such as fire resistance.

References

[1] U. N. E. Programme, "Global status report for buildings and construction: Towards a zero-emission, efficient and resilient buildings and construction sector," United Nations Environment Programme, Nairobi, Tech. Rep., 2021.

[2] N. Watson, "Lean design: 10 things to do now," *The Structural Engineer: journal of the Institution of Structural Engineer*, vol. 98, no. 8, pp. 12–14, 2020.

[3] T. Scheffler, "Development and application of precast hyperboloid shells in east and west germany from the 1950s to the 1980s," in *Proceedings of IASS Annual Symposia*, International Association for Shell and Spatial Structures (IASS), 2017.

[4] M. Dombrowski, P. Merz, J. P. Osman-Letelier, and M. Schlaich, "Transverse structural behaviour of doubly curved beam-like shells," in *Proceedings of IASS Annual Symposia*, International Association for Shell and Spatial Structures (IASS), 2020.

[5] M. Schlaich, A. Hückler, A. Goldack, and J. P. Osman-Letelier, "Vorgespannte flächentragwerke aus carbonbeton," in *Vielfalt im Massivbau – Festschrift zum 65. Geburtstag von Prof. Dr.-Ing. Jürgen Schnell*, 2018.

[6] J. P. Osman-Letelier, M. Schlaich, and A. Hückler, "Application of prestressed cfrp textiles for the development of thin-walled concrete structural elements," in *IABSE Congress New York City – The Evolving Metropolis*, 2019.

[7] M. Serrano-Mesa, J. P. Osman-Letelier, A. Hückler, and M. Schlaich, "Experimental investigation on prestressed thin-walled concrete folded slabs with CFRP textiles," in *Proceedings of IASS Annual Symposia*, International Association for Shell and Spatial Structures (IASS), 2020.

[8] M. J. J. Bucher, M. A. Kraus, R. Rust, and S. Tang, "Performance-based generative design for parametric modeling of engineering structures using deep conditional generative models," *Automation in Construction*, vol. 156, pp. 105–128, 2023.

[9] A. Eiz Eddin *et al.*, "Building acoustic analysis of doubly curved beam-like shells with CFRP prestressed concrete and its integration into an interdisciplinary optimisation tool," *Proceedings of IASS Annual Symposia*, 2024.

[10] S. Perse, N. Will, and J. Hegger, "CFK-vorgespannte Fußgängerbrücken aus Carbonbeton in Systembauweise - Vorbemessung und experimentelle Untersuchungen," in *HighTechMatBau-Konferenz*, 2018.

[11] J. Otto and R. Adam, "Carbonbeton und Stahlbeton im wirtschaftlichen Vergleich - Textile-reinforced concrete and reinforced concrete in an economic comparison," *Bauingenieur*, vol. 2019, pp. 246–252, Jun. 2019.

[12] R. Vierlinger, "Octopus - Generative Design in Architectural Engineering," Ph.D. dissertation, Jun. 2022.

[13] Bundesministerium für Wohnen, Stadtentwicklung und Bauwesen, *ÖKOBAUDAT - Datenbank für die Ökobilanzierung von Bauwerken*. [Online]. Available: `https://www.oekobaudat.de/no_cache/datenbank/suche.html`.

[14] Sirados Baudaten und Software. [Online]. Available: `https://www.sirados.de/`.

[15] ift Rosenheim GmbH, *Environmental Product Declaration (EPD) solidian GRID & solidian REBAR*, online, Dec. 2022. [Online]. Available: `https://solidian.com/wp-content/uploads/2023-05-25_ift-EPD-SGR-GB-65.0_solidian_EN.pdf`.